Journal of Cultural Heritage 77 (2026) 439–452

Contents lists available at ScienceDirect

Journal of Cultural Heritage

journal homepage: www.elsevier.com/locate/culher

VSI: TechnoHeritage2024

Multianalytical approach to the study of polymeric materials under artificial aging: Reference database

Ruth Chércoles Asensio[a,*], María Matesanz Benito[a], Marta Pérez Estébanez[a], María Higueras[a], Silvia G. Fernández-Villa[a], Sonia Santos Gómez[a], Elena Gómez-Sánchez[a,b], y Margarita San Andrés Moya[a]

[a] Faculty of Fine Arts, Complutense University of Madrid, Spain
[b] Deutsches Bergbau-Museum, Bochum, Germany

ARTICLE INFO

Article history:
Received 21 March 2025
Accepted 28 December 2025

Keywords:
Conservation
Restauration
ResinKit
Polymers
Database
PVC
Cellulose acetate

ABSTRACT

The accurate identification of polymeric materials used in Cultural Heritage is crucial for ensuring their preservation. Their inherent variability makes the identification and characterization a complex endeavor. Consequently, it is vital to improve identification methods and to deepen the understanding of plastic degradation. A comprehensive approach incorporating reliable reference standards is essential for the precise diagnosis of their state of conservation and to support appropriate intervention strategies and criteria. Furthermore, facilitating the dissemination of these data for practical application within the scientific and professional community is fundamental.

The primary objective of this study is to translate the aforementioned knowledge into a readily accessible resource in the form of a reference database providing a framework for the identification and conservation of polymeric heritage items and artistic production and assisting in the study of existing products on the market.

This research systematically analyses 50 widely used materials processed under the same conditions provided by The ResinKit™. The polymers were characterized using a range of analytical methods, including optical microscopy, spectrocolorimetry, Fourier Transform Infrared Spectroscopy Attenuated Total Reflectance (ATR-FTIR), and Pyrolysis-Gas Chromatography/Mass Spectrometry (Py-GC/MS). The samples were then subjected to artificial aging under controlled conditions of radiation (Xenon-Arc chamber for 1080 h), temperature and humidity (Climate test chambers for 840 h). The evaluation of the results was undertaken by repeating the series of previous tests and comparing them with the pre-aging analytical data.

The final step was to integrate all the results into a freely accessible online database that compiles all the information providing controlled reference standards for analyses of cultural artifacts and commercially available polymeric materials, thereby facilitating research in laboratories dedicated to the study of these materials within the context of fine arts and heritage conservation.

This paper analyses, as a case study, key heritage polymer families: polyvinyl chlorides (PVCs) and cellulose acetates (CAs).

1. Introduction

The mid-20th century's rise of macromolecular chemistry facilitated polymeric material use in cultural heritage and contemporary art [1]. However, these materials, not initially designed for such applications, can cause adverse effects [2]. Synthetic polymers may degrade, influenced by their chemical makeup, additives, processing, and environmental interactions [3]. Given diverse processing and additive techniques, long-term behavior information is often lacking [1,4,5]. Thus, composition, properties, stability, and compatibility investigations are crucial for conservation [6].

A considerable number of studies on this topic have emerged in recent decades [7–10]. Research initiatives like POPART [11] a and POLYEVART [5,12] address polymer instability, fostering new material development. Online libraries, such as the Spectral Database of The Infrared and Raman User Group (IRUG), only provide spectral

* Corresponding author at: Faculty of Fine Arts. Complutense University of Madrid, C/ Pintor El Greco, 2, 28040, Madrid, Spain.
E-mail address: rmcherco@pdi.ucm.es (R.C. Asensio).

https://doi.org/10.1016/j.culher.2025.12.013

references, though aged material data is limited. Despite advancements, material identification remains challenging due to insufficient reference patterns, hindering result interpretation and long-term behavior comprehension [13].

Cultural heritage material complexity demands robust reference patterns, as computer matching programs struggle with complex or degraded samples, lacking spectral library models. This highlights the ongoing need for improved reference databases and analytical techniques to ensure effective conservation strategies [14].

Given the diversity of polymers, there is a need for accessible collections of materials processed under controlled conditions, which can serve as reference patterns for conservation laboratories and which contain multiple compilation data with relevant and structured information on their evolution and degradation over time.

In this article, as a demonstration of the practical application, the results of two families of polymers quite relevant within the cultural heritage, CAs and PVCs, are presented. Both are fragile in the medium and long term, so must be preserved in the best possible condition [15–17].

PVC is a widely used, affordable, and versatile polymer found in multiple heritage contexts, including artifacts like sculptures, toys and furniture [1], protective materials like photographic supports [5,18], and audiovisual media such as vinyl records and magnetic tapes [19]. Cellulose acetates and other mixed esters with butyrate and propionate, are semi-synthetic polymers that have been also used for years in industrial, commercial and artistic products. They have been used as film supportand constitute the basis of historical audiovisual heritage and form the physical stock of original tapes [20,21].

The selection of these polymers was determined by the observed significance of their degradation pathways-encompassing both physical and chemical properties during artificial aging-which provides practically applicable information regarding material evolution for conservators, restorers, and artists.

2. Research aim

The present work proposes a systematic study of polymeric materials that have undergone similar injection molding processing without colorants. The primary objective is the creation of a practical, freely accessible online reference database for the study of the long-term behavior of polymeric materials used in the fields of conservation, restoration and artistic production, thus facilitate the study of existing products on the market.

The proposed methodology is meticulously designed for the heritage sector, founded on the analysis of fundamental physical and chemical properties to characterize and predict the long-term behavior of polymers. This approach is achieved by selecting low-variability polymer standard references (ResinKit™) and focusing on key properties, such as color, that are specifically chosen for their critical relevance to conservation-restoration. The resulting data, including deterioration patterns and stability reference standards, are crucial for practical heritage application and are made available to a wide range of professionals within the field. This information ultimately guides the selection of compatible materials and the establishment of optimal preventive and corrective conservation strategies.

3. Materials and methods

The methodology employed comprises several steps, starting with the material selection. It is founded on the comparison of a range of key physical and chemical properties before and after the artificial aging in different conditions of temperature, relative humidity (RH) and radiation. This enables the characterization and prediction of the long-term behavior of polymers [22].

The methodology is constituted by the following steps (Fig. 1):

3.1. Material selection

A total of 50 polymers supplied by The ResinKit ™ (Woonsocket, RI, USA) were subjected to a systematic analysis (see Table S1). These polymers were processed through injection molding without colorants.

They are materials employed in artistic endeavors, including the creation of artistic works, as well as associated elements such as exhibition stands, packaging, conservation and restoration materials, etc., showing thermoplastic or elastomers behavior. This is a representative compilation of polymeric materials that have been used as reference standards in various research projects in cultural heritage [27,28].

The samples studied were obtained from the chips included in ResinKit, which were cut into 4.5 × 1.5 cm plates and rods of 2 cm length and 2 mm diameter. After analyzing the kit, the accurate allocation and labelling indicated by the manufacturer was confirmed.

3.2. Property selection

3.2.1. Physical properties: analytical techniques and equipment

This study has addressed the physical characterization of the materials through a range of methods, including morphological study, dimensional analysis, gravimetry, thermal properties and color analysis (Fig. 2). Mass changes were determined using an A&D Company, Limited ER-120A precision balance, Cal-100.0002. Dimensional variables (length, width and thickness) were obtained using a Qfun mod. BWK007 digital caliper with an accuracy of ±0.02 mm. Three measurements were made for each sample. The morphological examination was performed with a Leica MZ125 binocular microscope equipped with a Leica DC150 digital camera, and the macrophotographs were taken with a Nikon D3100 digital SLR camera in a light box. Thermal properties were obtained with a TA Instrument SDT-Q600 simultaneous thermogravimetric analysis/differential scanning calorimetry (TGA-DSC) equipment was used, applying a heating ramp of 10 °C/min from room temperature to 650 °C in an N_2 atmosphere and a platinum sample holder.

Color is a physical property susceptible to degradation processes in polymers and indicative of structural transformations in the material [3,17]. Color measurements were performed using a Konica Minolta CM-2600d spectrophotometer with a wavelength range of 400 nm-700 nm and a 10 nm interval. The instrument utilized a D65 standard illuminant (daylight with a color temperature of 6504 K) and the CIE 196410° standard observer. The optical geometry used was diffuse illumination/8° viewing (d/8) reflection. Measurements were carried out with the specular component included (SCI) and excluded (SCE), using a measuring area diameter of 3 mm. All colorimetric parameters were defined in CIE L*a*b* coordinates. Thresholds were established in accordance with international recommendations for the evaluation of color differences [23]. To ensure reproducibility, five color measurements are taken at specific points on each specimen using a template to guarantee the consistency of the measured area. The final reported value is the average of these five data points. For accelerated Xenon-Arc artificial aging, measurements are exclusively performed on the irradiated surface.

3.2.2. Chemical composition: analytical techniques and equipment

The chemical composition of the polymeric matrix and additives has been studied by ATR-FTIR and Py-GC-MS (Fig. 2). The

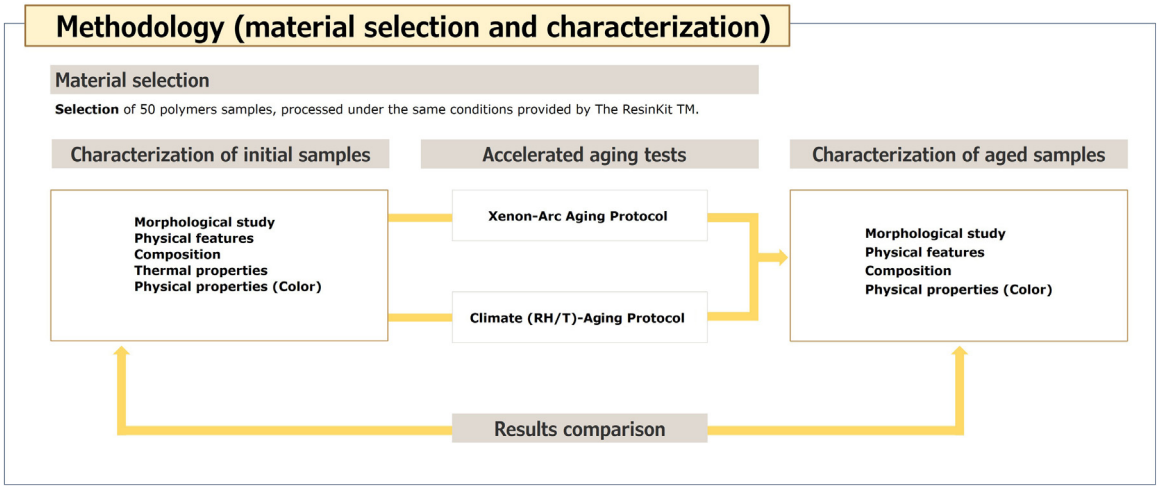

Fig. 1. Methodology overview.

combination of both techniques provides information of chemical composition and molecular structure of the polymer [24].

The ATR-FTIR measurements were obtained using a Thermo Nicolet 380 instrument associated equipped with a DTGS/KBr detector and an attenuated total reflection diamond crystal accessory. Spectra were recorded in the mid-infrared (4000 and 400 cm^{-1}) with a 4 cm^{-1} resolution and 32 scans.

Py-GC-MS analysis was performed using an Agilent Technologies 7890A Gas Chromatographer interfaced with an EGA/PY-3030D Multi-Shot Pyrolyzer and an Agilent Technologies 5975C Mass Spectrometer.

Pyrolysis was carried out in double shot (DS) mode (Py-GC/MS) at 600 °C. To help with the identification of volatile compounds such as plasticizers, a thermal desorption (TD) step was performed prior to pyrolysis. This involved increasing the temperature from 50 °C to 300 °C at a rate of 50 °C/min over a period of 6 min. The pyrolyzer interface temperature was set at 290 °C. The DS method is superior as it enhances sensitivity and resolution for complex polymer formulations by eliminating the co-elution of additives and polymer pyrolyzates common in traditional single-shot analysis.

The volatile products were introduced at GC via the Front Multi-Mode (MM) Inlet, which was maintained at 300 °C and operated in split mode with a 100:1 split ratio. Separation was achieved on an Agilent UA5-30m column (30 m x 250 µm x 0.25 µm) film thickness with 5 % Phenyl Methyl Polysiloxane. Helium was used as the carrier gas at a constant flow rate of 1 ml/min. The GC oven program was temperature ramp started at 40 °C (2 min), rise to 320 °C at 20 °C/min and maintained 15 min at 320 °C.

The mass spectrometer was operated in Electron Ionization (EI) mode at 70 eV energy. The MS temperatures were set as follows: MS transfer line (interface) 290° C and the ion source 230 °C, and quadrupole at 150 °C. Mass spectra were acquired in full scan mode from 29.0 to 550.0 *m/z*.

The mass spectral (MS) libraries used for polymer and additive identification were the PYGC-MS18B and ADD-MS16B (Frontier Laboratories).

3.3. Artificial aging

To evaluate and predict the long-term behavior of the samples, accelerated artificial aging tests were carried out in climatic chambers. Electromagnetic radiation (Xenon-Arc) and the combination of relative humidity (RH) and temperature (T) were chosen as the representative variables for use in polymer artificial aging tests [25]. To this end, two identical series of samples were prepared. The samples were arranged regularly on a foam board covered with a sheet of Melinex® polyester to prevent any interaction between the samples and the support.

The protocols, depicted in Tables S2a and S2b, were designed in accordance with the directives stipulated by the UNE-EN ISO 4892-2 and ISO 9142:2003 that are appropriate for their use in research on the conservation field [26,27].

A Suntest XLS+33 Xenon-Arc solar simulation chamber with three air-cooled Xenon-Arc lamps with irradiance control was used. It has a window filter that eliminates UV radiation below approximately 320 nm, to simulate exposure through 3 mm thick glass (museums indoor). Five light cycles of 300–400 nm were applied with a total accumulated irradiation of 1080 h plus 168 h in darkness, and temperature conditions of 60 °C and an irradiance of 60 W/m^2.

The climate artificial aging process (RH/T) was conducted in a Vötsch Neurteck climatic chamber model VCL 4010. Five cycles of 168 h were carried out with variable relative humidity levels ranging from 90 % to 30 % and temperature settings between 23 °C and 55 °C.

3.4. Comparative study

Samples subjected to artificial aging cycles under the established conditions, were then studied with the same techniques defined in the characterizations study. Intermediate measurements were made at the end of each cycle (designated t_0 for the initial state and C1–5 for the number of each cycle) except Py-GC-MS since it is a destructive analysis technique. It is important to note that, in the case of accelerated artificial aging by Xenon-Arc, measurements were always carried out on the irradiated side.

Finally, a comparative study of the results obtained during accelerated artificial aging and the initial characterization data at time zero is performed.

4. Results and discussion

All data collected during the experimental phase is collated and organized (Fig. 2) in an online database, which is freely accessible. This format enables straightforward access to the data through simple searches. The database has been designed with an intuitive, clear and user-friendly interface to appeal to a diverse range of users. However, emphasis has been placed on ensuring the database is rigorous and appropriate for its use among heritage

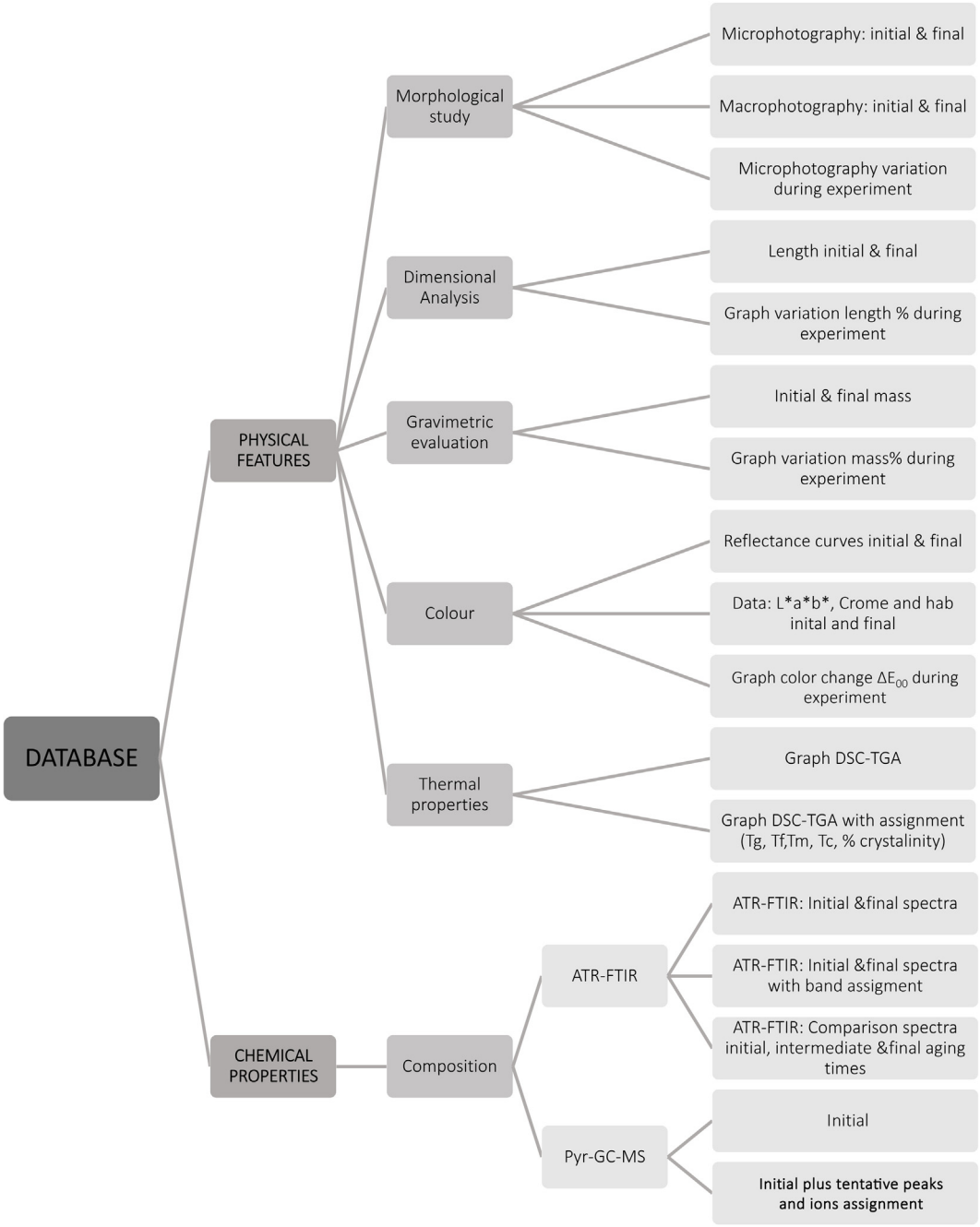

Fig. 2. Graphical representation of the results showed in the database according to the property under study and the selected technique.

professionals and scientists. The database is available since January 2025: https://proyecto-resinkit.labmat-ucm.com/.

Two case studies are considered to understand the practical use of the database. In the following, the analysis procedure (identification and artificial aging) and the results of two distinct polymeric families: PVCs and CAs, are presented and discussed. In both families, the most evident alterations of the materials were observed under Xenon-Arc radiation. These conditions will be the primary focus of the ensuing discourse.

4.1. PVCs

4.1.1. Identification

The PVC samples studied here were obtained from two ResinKit chips, which are referred to using the manufacturer's designations: 29 PVC-Flexible and 30 PVC-Rigid. According to the manufacturer, these samples possess analogous polymeric matrices and differ in their elastic properties.

The ATR-FTIR spectra show, in both cases, the most significant bands of PVCs related to the chlorinated polymeric chains as well as bands corresponding to the plasticizers and additives added during the manufacturing process (Figure S1 and Table S3).

Bands attributable to aliphatic C–H groups were observed, corresponding to stretching vibrations in the range of 2925–2856 cm^{-1} and at 741 cm^{-1}, as well as wagging vibrations around 1425 and 1273 cm^{-1}. Additional bands associated with CH_2 groups were identified, corresponding to symmetric and asymmetric stretching vibrations in the 2925–2856 cm^{-1} region and to bending vibrations near 1425 cm^{-1}. Furthermore, contributions due to C–Cl stretching vibrations were detected in the range of 690–607 cm^{-1}. Both poly-

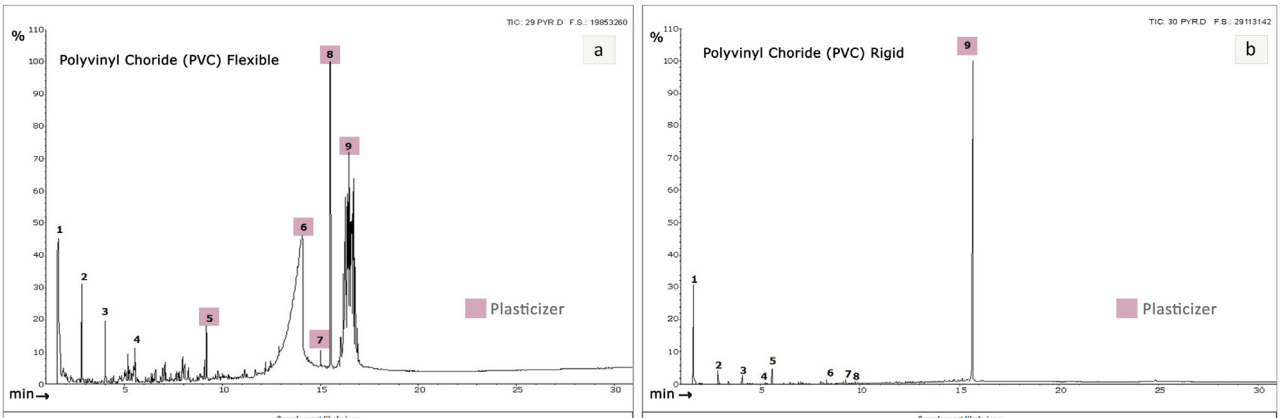

Sample most likely ions

No.	Retention time (min)	Compound	MW	M/Z
1	1,61	Hydrogen chloride	35	30,36
2	2,79	Benzene	78	50,5152,77,78
3	6,80	Toluene	92	39,51,65,91
4	5,53	p-Xylene	106	39,51,55,65,77,91,106
5	9,13	Phthalic anhydride	148	50,76,104,148
6	14,08	Terephthalic acid	166	50,65,74,121,149,166
7	15,02	Triphenyl phosphate (TPP)	326	39,51,65,77,94,149,465,215,326
8	15,52	Bis(2-ethylhexyl) phthalate (DEHP)	390	29,43,57,71,149,167,279,390
9	16,77	Diisononyl phthalate (DINP)	418	57,71,149,293

Sample most likely ions

No.	Retention time (min)	Compound	MW	M/Z
1	1,61	Hydrogen chloride	35	30,36
2	1,9	Benzene	78	50,5152,77,78
3	2,52	Toluene	92	29,31,43,45,60,
4	5,20	p-Xylene	106	39,50,51,63,65,77,91,92
5	5,55	Styrene	104	39,51,78,103,104
6	8,32	Naphthalene	128	32,39,41,43,55,60,71,87,101,126
7	9,17	2-Methylnaphthalene	142	41,51,63,71,91,115,129,142
8	9,73	Acenaphthene	154	51,63,76,102,115,128,143,154
9	15,65	Bis(2-ethylhexyl) phthalate (DEHP)	390	29,43,57,71,149,167,279,390

Fig. 3. Pyrograms of the materials and most probable mass/charge (*m/z*) ions found at time zero: a) PVC-Flexible b) PVC-Rigid.

mers show a sharp band at 3675 cm^{-1} which can be attributed to the OH groups of the water of crystallization of kaolinite added as filler.

The FTIR-ATR spectrum reveals the presence of absorption bands attributable to plasticizing additives such as phthalates. A distinct band at 1722 cm^{-1} corresponds to the symmetric and asymmetric stretching vibrations of the C=O group. Additionally, bands observed at 1122 and 1070 cm^{-1} are associated with the stretching vibrations of the C–O bond. Furthermore, the presence of an absorption band corresponding to the C=C stretching of the aromatic ring is also evident. These bands exhibit greater intensity and clarity in the PVC-Flexible sample compared to the PVC-Rigid, which can be attributed to the higher content of phthalic acid-derived plasticizers present in what the manufacturer refers to as flexible PVC, as opposed to the rigid formulation.

Fig. 3 displays the obtained pyrograms and the identified products. While HCl, benzenes, toluenes, and naphthalenes were identified in both PVC samples, the PVC-Flexible spectrum also exhibited several prominent peaks. These peaks were also observed in the TD chromatograph, and correspond to plasticizer compounds, including phthalates (such as Di-'isononyl' phthalate (DINP) and Bis (2-ethylhexyl) phthalate (DEHP)) and phosphates, specifically triphenyl phosphate (TPP), which is additionally known to function as a flame retardant.

The most intense peak corresponds to DEHP, and it is, conversely, the only one detected in the PVC-Rigid. Its content can reach, according to the literature, 30–50 % by weight [28,29]. Phthalic acid esters, once prevailing plasticizers due to their low cost and effectiveness, are now significantly restricted due to their negative impacts on human health and the environment [28].

4.1.2. Artificial aging

Artificial aging with Xenon-arc radiation revealed a different behavior of both materials (Figs. 4 and 5). At a macroscopic level, the PVC-Rigid is progressively altered until it was severely degraded at the end of the experiment. Both mass and dimension decrease in parallel, with deterioration accelerating from cycle 2 (C2) (Fig. 4a). Approximately 6 % of the total weight and 3 % of the length were lost. The loss of mass and dimensions can be attributed to the exudation or evaporation of the plasticizer.

This process is accompanied by a gradual color change that accelerates in the final three cycles to a total darkening of the surface (Fig. 4b), which translates into a progressive and marked increase in the slope of the variation of the yellowing index (ΔE_{00}) with a maximum after cycle 3 (Fig. 4b). This color change is further evidenced in the CIE L*a*b* diagram (Fig. 4d) with a highly saturated orange hue that transitions to browns with minimal chroma from the third cycle onwards. At this point, the color variation (ΔE_{00}) stabilizes, and the most notable change is the loss of luminosity L*, approaching values close to black at the end of the artificial aging test. These variations can be attributed to oxidation and dehydrochlorination processes and the creation of polyene groups with conjugated bonds that absorb at different wavelengths [29]. Dehydrochlorination is an autocatalytic reaction; that is, if the hydrogen chloride produced is not removed from the PVC environment, dehydrochlorination continues at an accelerated rate [30].

In the case of PVC-Flexible, in the initial stages, the material's opacity increases, but no yellowing or substantial variation in mass and length is observed (Fig. 4a). The material's characteristics remain relatively stable until the third cycle, at which point degradation occurs abruptly, accompanied by acute yellowing (Figs. 4b and c). This change is also macroscopically perceptible (Fig. 5). Subsequently, there is an intense darkening in the periods C4 and C5, accompanied by a decrease in luminosity to levels similar to those observed in PVC-Rigid (Fig. 4c). Simultaneously, a decrease in weight and a rapid dimensional distortion is observed with a reduction of 14 % of its mass and a contraction of 6 %, which is almost double that of PVC-Rigid (Fig. 4a).

It is difficult to determine the individual effects of the polymeric matrix and the plasticizers on the stability of the material, given the feedback and synergistic reactions they produce. The existing literature indicates that the PVC matrix is more sensitive to thermal decomposition than plasticizers [31] and at room temperature the latter reduce the rate of dehydrochlorination of PVC [32].

It can be hypothesized that the presence of plasticizers in PVC-Flexible has temporarily mitigated the alterations by inhibiting the growth of polyene sequences. For example, the ester groups of plasticizers dissolve the labile groups of the polymeric chain responsible for instability, thereby preventing the formation of double bonds [32]. However, when this capacity is lost by being exuded or removed from the sample, degradation begins very quickly. This could explain the behavior of PVC-Rigid with a much smaller proportion and variety of plasticizers than PVC-Flexible.

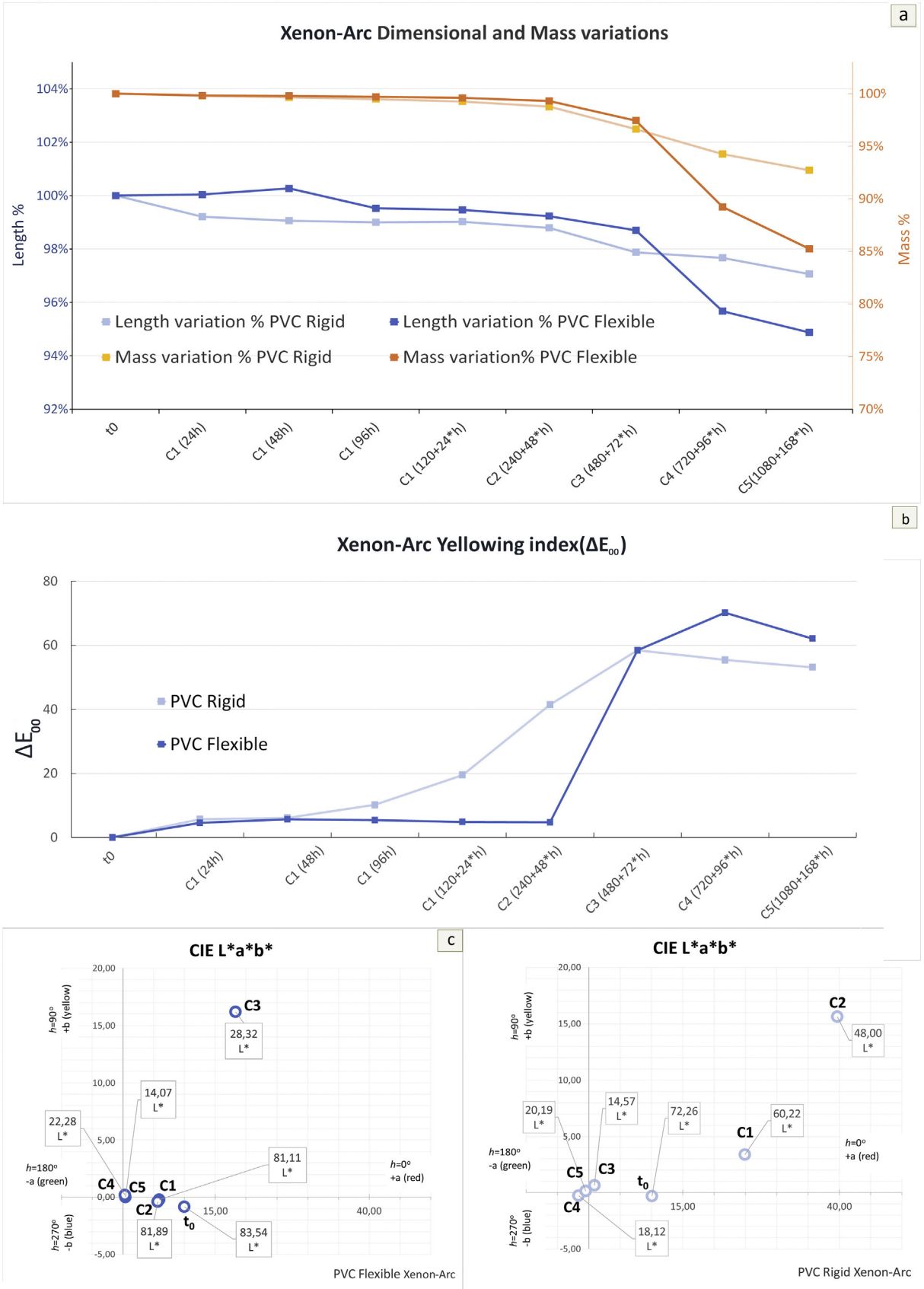

Fig. 4. Gravimetric-dimensional and colorimetric study versus artificial aging time under Xenon-Arc radiation of samples PVC-Flexible and PVC-Rigid. a) Variation in length and mass. b) Color Variation: yellowing index c) CIE L*a*b* diagram of PVC-Flexible and d) CIE L*a*b* diagram of PVC-Rigid.

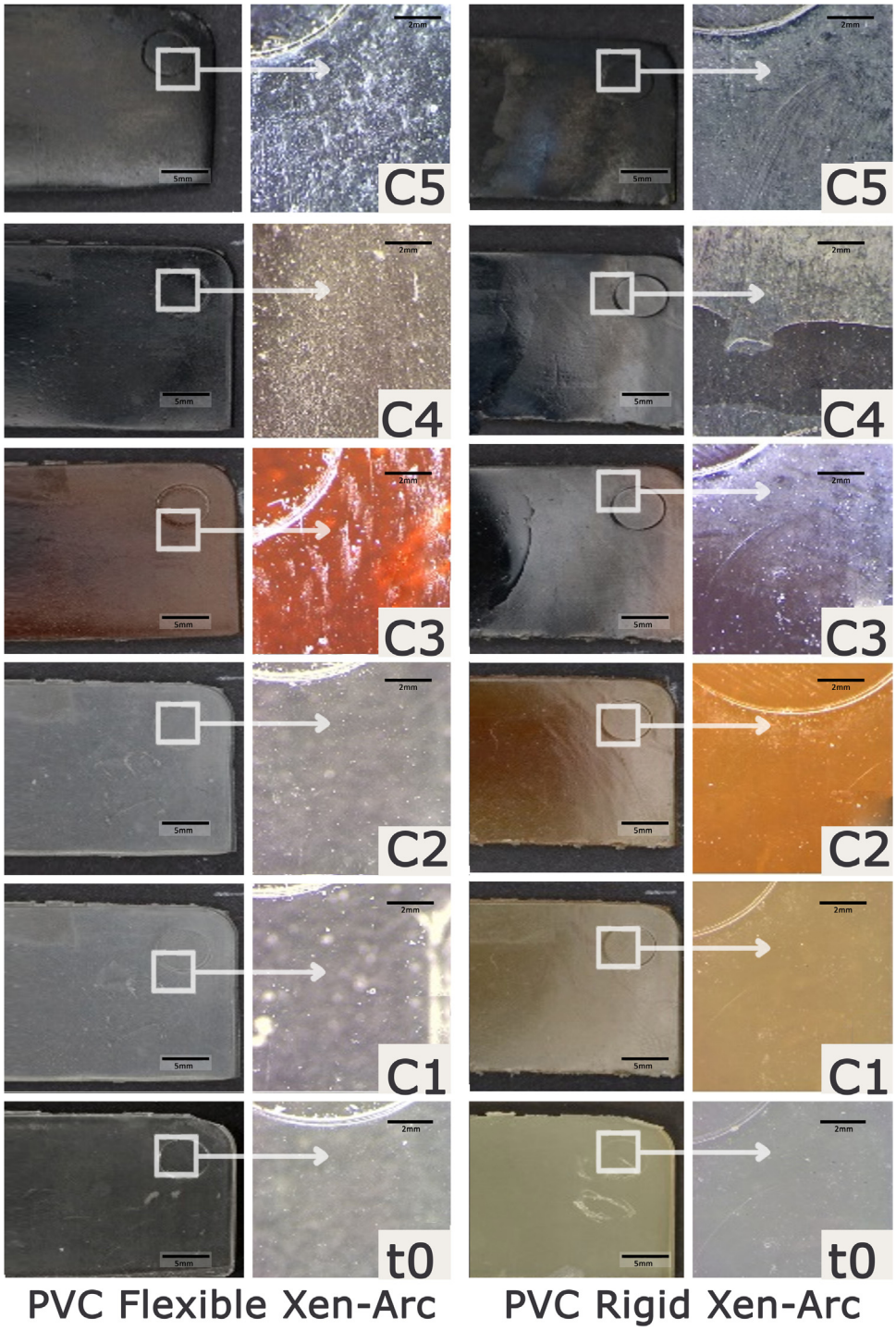

Fig. 5. Macro and microphotographs (x2.5) of samples PVC-Flexible and PVC-Rigid. Artificial aging-time variation under Xenon-arc radiation.

This can be seen very well both in the pyrogram and in the thermal desorption chromatogram (latter not shown but comparable to the former), where the simplicity of the PVC-Rigid chromatograms strikes against the complexity and breadth of plasticizer-related peaks from the PVC-Flexible.

The ATR-FTIR spectra after artificial aging, showed that Xenon-Arc radiation produces significant variations in both materials, starting from the first cycle. These variations became discernible from the third cycle and intensify at the end until completely blurring the characteristic spectrum of PVC.

As it is seen in Fig. 6, within the wavenumber range between 3000 and 2800 cm^{-1}, the stretching vibration bands of the C–H bond corresponding to the CH–Cl groups (2956 cm^{-1}) and CH_2 (2956–2856 cm^{-1}) cannot be detected. Additionally, the bands of C–H bonds (1425,1378–1273 cm^{-1}) become broad, hindering clear distinction. All these changes confirm the degradation process of the polymeric chains as previously outlined. Furthermore, the emergence of a broad band around 1600 cm^{-1} is observed, which corresponds to the stretching vibration of the conjugated double bonds that form within the main chain as a consequence

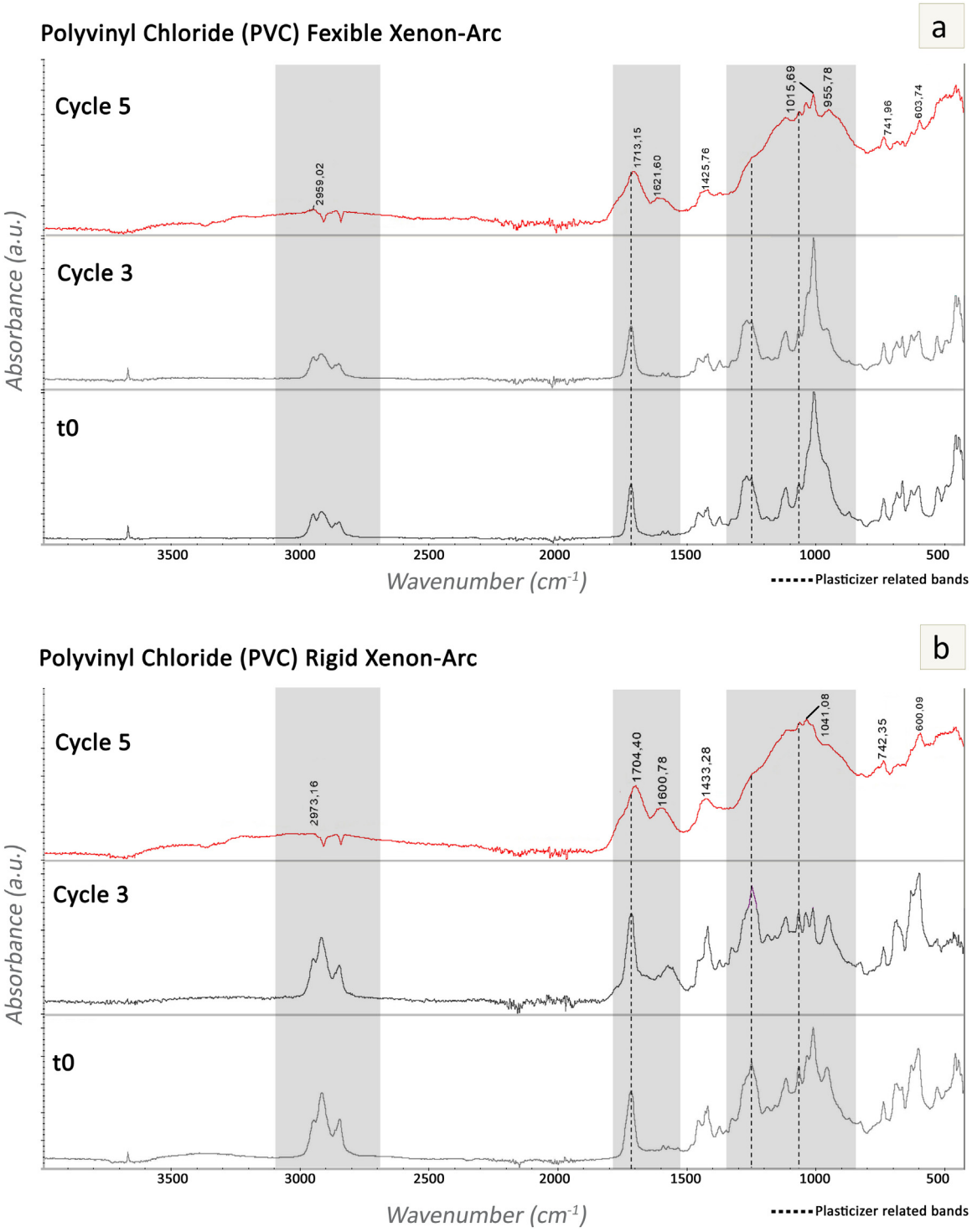

Fig. 6. ATR-FTIR spectra observed in the initial, intermediate (C3) and final(C5) stages of artificial aging experiment under Xenon-Arc radiation. a) PVC-Flexible. b) PVC-Rigid.

of its degradation. This effect occurs from cycle 3 in PVC-Rigid and in cycle 5 in PVC-Flexible, in agreement with the different behavior of the physical properties observed and indicating an earlier deterioration of PVC-Rigid.

Alternatively, a decrease and shift towards lower wavelengths of the band associated with the carbonyl group (C=O) (1722 cm^{-1}) and those of the C–O groups (1122 and 1073 cm^{-1}) is observed, which indicates the loss of plasticizer during the artificial aging process. In addition, the appearance of a broad band near the C=O region suggests the formation of multiple functional groups, including acids and ketones [29].

Conversely, the spectra of the two PVC materials are similar after artificial aging, which indicates that degradation in both cases has occurred via a comparable mechanism.

The chemical changes associated with the processes of photo-oxidation and degradation of PVC cause variations in color, mass and dimension, as evidenced by the colorimetric measurements and the morphological-physical study.

In relation to the artificial aging process in conditions of humidity and temperature (see Figures S2-S3-S4), no variations are observed in the dimensional or gravimetric parameters. However, some changes in the ATR-FTIR spectra are observed, especially in the fingerprint region, indicating the beginning of their degradation. At a macroscopic level, this translates into yellowing that is reflected in the color variation graphs. In PVC-Rigid these alterations are more pronounced, though less significant than those observed in samples exposed to radiation.

4.2. Cellulose acetates

4.2.1. Identification

The samples studied come from the ResinKit Chips: 11 Cellulose Acetate (CA), 12 Cellulose Acetate Propionate (CAP) and 13 Cellulose Acetate Butyrate (CAB).

The ATR- FTIR spectra of the three samples are very similar (Figure S5), with the main differences in the regions of CH_2 stretching (3000 - 2840 cm^{-1}) and bending (1365 cm^{-1}) and C–O-C stretching (1160–1039 cm^{-1}) [33]. The observed spectral characteristics are attributable to the incorporation of esterifying acids with a higher number of carbon atoms [33], such as butyric or propanoic acid, and, to a lesser extent, to the contribution of plasticizers.

The stretching vibration of the carbonyl group (C=0) appears around 1738 cm^{-1} in the three acetates. Meanwhile, symmetric and asymmetric vibrations of the C–O–C bond are observed around 1160 and 1030 cm^{-1} respectively, with a minor shift of the asymmetric vibration in CAP towards higher wavelengths (1060 cm^{-1}). Furthermore, the most significant differences appear in the area of the asymmetric tension (C–C–O) of the ester. CA has an intense band around 1214 cm^{-1}, CAB presents a characteristic double peak at 1225–1159 cm^{-1}, and CAP shows a very strong band at 1158 cm^{-1}. However, the band corresponding to the 1200 cm^{-1} region is barely perceptible and appears as a shoulder [33,34].

In contrast, the vibration bands of CH stretching at 3000–2850 cm^{-1} are discernible in both CAP and CAB, though they are less pronounced in CA. Regarding the CH bending vibrations around 1365 cm^{-1} observed in mixed acetates, these bands exhibit greater width and the potential to divide into multiple bands, as evidenced in CAP [35].

The presence of additives such as triphenyl phosphate and phthalates is indicated by the presence of other smaller bands located at 1599–1589 cm^{-1} (C=C stretching aromatic ring), 1460 (CH bending) and 900 cm^{-1}(CH bending/ aromatic ring) [34].

The analysis by Py-GC-MS (Fig. 7) confirms the different acetylated esters of cellulose and the presence of plasticizers.

The peaks corresponding to the short-chain organic acids, which are produced from the pyrolytic decomposition of the side chains of the polymer: acetate, butyrate and propionate, and which define each ester, appear at short retention times (between two and six minutes) and are poorly resolved. The peaks of the plasticizers, by contrast, appear after nine minutes and are more intense and well-defined, since these compounds evaporate easily and do not normally decompose at pyrolysis temperatures [34]. The presence of DEHP has been identified in all cases and DEP in CA and CAP (in the latter, in traces amount only visible in the TD chromatograph,). Furthermore, trace quantities of TPP have been detected in CAB and CA, bis (2-ethylhexyl) azelate in CAB and bis (2-ethylhexyl) adipate in CA.

4.2.2. Artificial aging

It should be noted that cellulose acetates are particularly sensitive to humidity. In environmental conditions with high RH-T, the phenomenon known as “vinegar syndrome” occurs. This phenomenon involves the deacetylation by hydrolysis of the polymeric

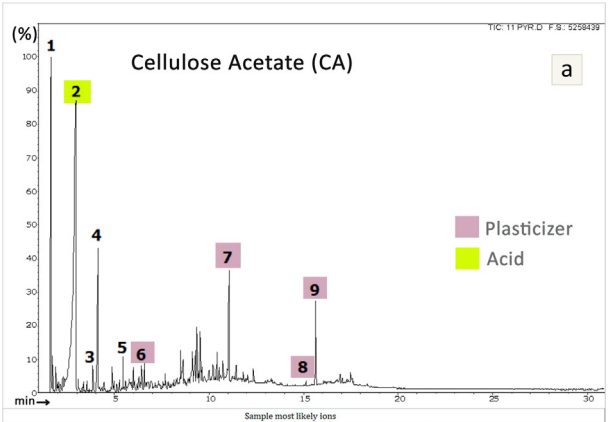

Sample most likely ions

No.	Retention time (min)	Compound	MW	M/Z
1	1,61	Carbon dioxide	44	44
2	2,93	Acetic acid	60	29,31,43,45,60,
3	3,87	2-Methylfuran	82	29,39,50,51,53,54,55,81,82
4	4,12	2-Hydroxyethyl acetate	104	29,31,42,43,73,103
5	5,49	4-Cyclopentene-1,3-dione	208	39,44,51,65,77,91,115,117,208
6	6,43	Phenol	94	39,43,55,66,82,94
7	11,06	Diethyl phthalate (DEP)	222	43,65,76,93,105,149,177,222
8	15,13	Triphenyl phosphate (TPP)	326	43,77,149,169,215,233,326
9	15,63	Bis(2-ethylhexyl) phthalate (DEHP)	390	29,43,57,71,149,167,279,390

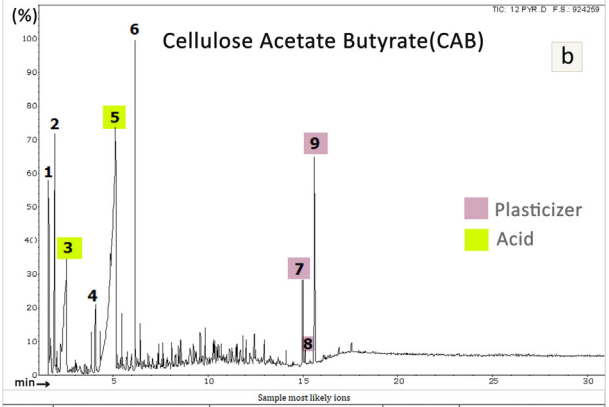

Sample most likely ions

No.	Retention time (min)	Compound	MW	M/Z
1	1,58	Carbon dioxide	44	44
2	1,9	2-Methyl-2-butene	70	30,37,39,40,41,42,55,70
3	2,52	Acetic acid	60	29,31,43,45,60,
4	4,07	2-Hydroxyethyl acetate	104	29,31,42,43,73,103
5	5,14	n-Butanoic acid	88	29,39,42,45,60,73
6	6,16	Acetic butyric anhydride	130	39,41,43,55,60,71,87,101,126
7	15,00	Bis(2-ethylhexyl) adipate	370	41,57,70,83,112,129,147
8	15,13	Triphenyl phosphate (TPP)	326	43,77,149,169,215,233,326
9	15,63	Bis(2-ethylhexyl) phthalate (DEHP)	390	29,43,57,71,149,167,279,390

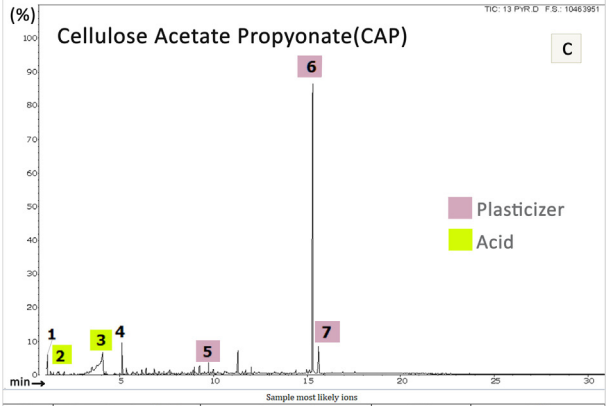

Sample most likely ions

No.	Retention time (min)	Compound	MW	M/Z
1	1,13	Acrolein	56	29,37,39,41,54,55,56
2	1,78	Acetic acid	60	29,31,43,45,60,
3	4,07	Propionic acid	74	30,45,55,57,70,73,74
4	5,12	Hydroxy-2-butanone?	88	29,42,57,88
5	9,26	Phthalic anhydride	148	50,76,104,148,
6	15,32	Bis(2-ethylhexyl) azelate	148	50,76,104,148,
7	15.63	Bis(2-ethylhexyl) phthalate (DEHP)	390	29,43,57,71,149,167,279,390

Fig. 7. Pyrograms of the materials and most probable mass/charge (m/z) ions found at time zero: a) CA, b) CAB c) CAP.

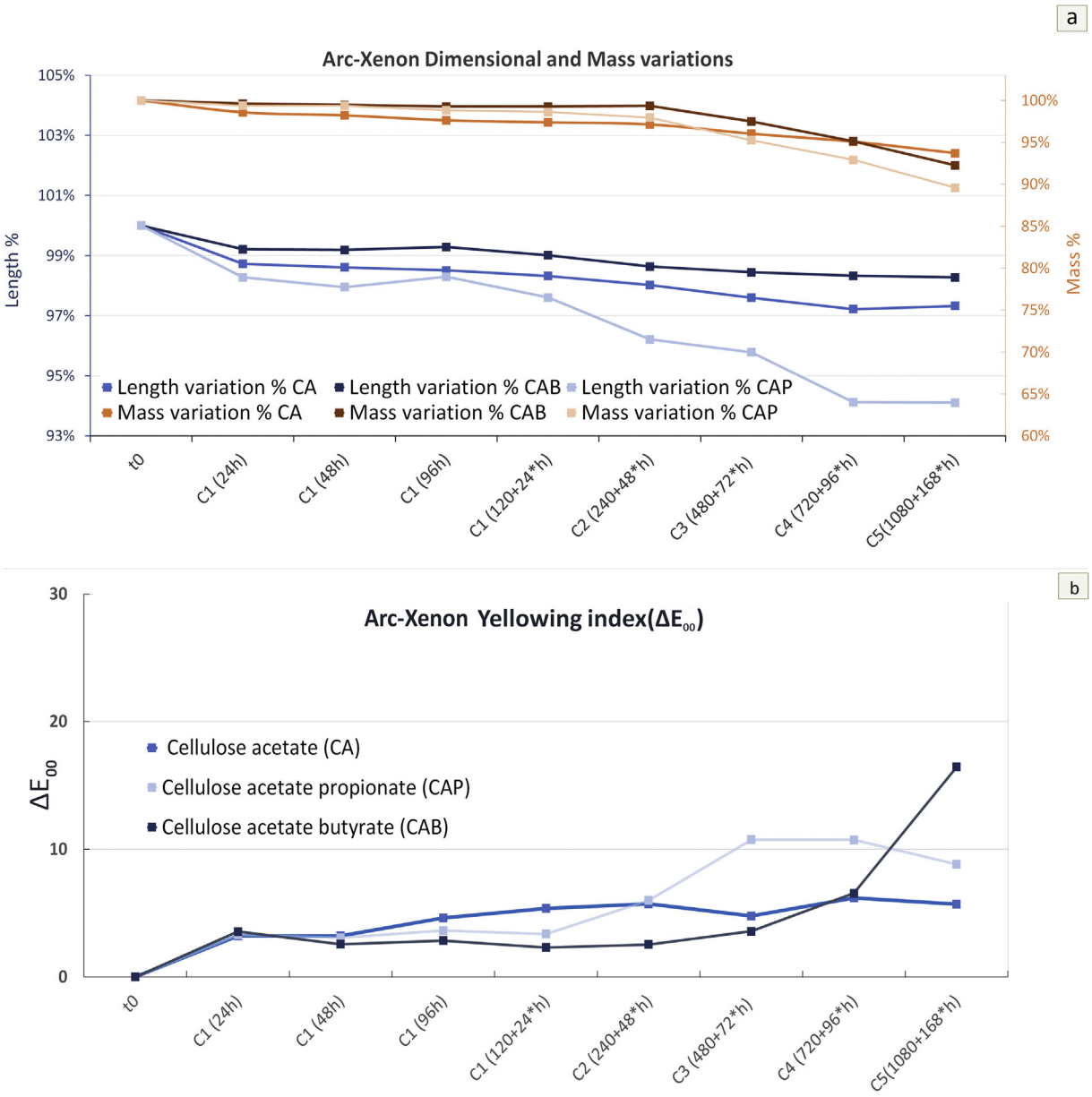

Fig. 8. Gravimetric-dimensional and colorimetric study versus artificial aging time under Xenon-Arc radiation of CA, CAB and CAP; a) Length and mass Variation. b) Color Variation: yellowing index.

chain, resulting in the release of acetic acid and subsequent reversion to cellulose [34,36,37]. However, during the artificial aging test with the RH-T conditions employed in this study, the materials exhibited no substantial response. Instead, they remain unaltered or presented less alteration compared to the artificial aging test with radiation.

Artificial aging with Xenon-Arc radiation has produced, in the three materials, dimensional oscillations, loss of mechanical integrity and changes in the visual appearance (Figs. 8, 9).

A loss of mass between 5 and 10 % is evident in the three acetates from cycle 2, exhibiting CA the smallest variation. Additionally, a contraction of the samples is observed, gradually, and more pronounced in CAP. The reduction of these two magnitudes could be associated with the loss of the plasticizer by evaporation.

The migration and evaporation of plasticizers have also been demonstrated to result in their friability [38,39]. This phenomenon has been corroborated through experimental observation, which has revealed an increase in the rigidity and fragility of the samples. The loss of mechanical resistance has been observed to cause CAP to fracture in C3 and CAB in C5. In contrast, CA does not fracture after artificial aging, although a pattern of striae or channels is evident. In the case of CAB, the presence of bubbles containing crystals has also been noted (Fig. 9).

If we assume the reduction of mass is entirely attributable to the loss of plasticizer, in the case of CAP it would correspond to practically all the plasticizer present, given the percentages normally used in its manufacture (10–15 %). On the contrary, the degradation of CA retains a greater amount of plasticizer, since it usually has a higher initial percentage (10–35 %) [40].

The presence of TPP may be a risk factor to its recrystallization [41] However, in this case it is the polymer that did not present this component, the CAB, the most affected during artificial aging, possibly because this plasticizer is less volatile than other phthalates such as DEP [36]. On the other hand, the di-n-hexyl adipate

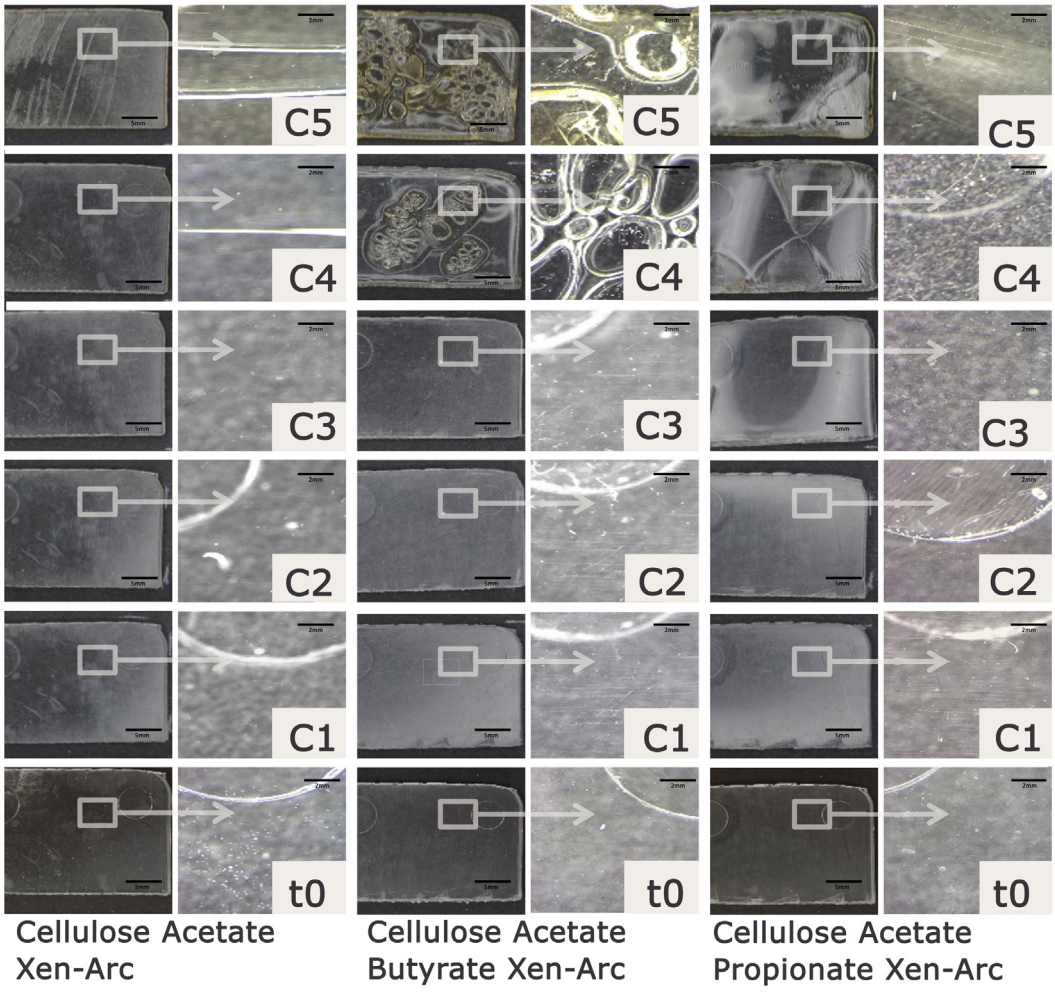

Fig. 9. Macro and microphotographs (x2.5) of samples CA, CAB and CAP artificial aging-time variation under Xenon-arc radiation.

present in CAB is characterized by its resistance to water and non-volatility [33,42], which may have mitigated the loss of mass and contraction of this material.

In relation to the occurrence of yellowing in CA, this parameter remains stable with a slight increase as the exposure time increases. At the end of the first cycle, an increase in ΔE_{00} is already evident in CAP, which subsequently stabilizes in C3. Conversely, CAB remains unaltered until the third cycle, when visible yellowing begins, resulting in a significant increase in the slope of the curve, particularly in the last artificial aging cycle (Fig. 8b).

ATR-FTIR spectra have revealed the chemical variations caused during the artificial aging with Xenon-Arc radiation (Fig. 10). In the three materials, an enhancement in the broad band corresponding to the vibration of the OH groups around 3500 cm^{-1} is discerned. Likewise, an increase in the intensity of the band corresponding to the carbonyl group (1731 cm^{-1}) is distinguished accompanied by the emergence of a pronounced shoulder on its right. The presence of this band indicates the formation of multiple functional groups, which can be attributed to the degradation of the material and the subsequent scission of the acetyl substituent groups [33,43–45]. The intensity of the remaining ester bands (CO and COC) also undergoes an increase.

The degradation mechanism of the ester side chain by hydrolysis is, by far, the most significant [34]. Not only does depolymerization change the polymeric matrix, but it also contributes to the degradation and emission of other compounds used in the manufacturing process such as plasticizers. This means that, at relatively low temperatures, the loss or evaporation of the plasticizer can occur [46]. The loss of plasticizer therefore intensifies degradation and artificial aging. [47]. Bands assigned to the plasticizer located at 1589, 1460 and 900 cm^{-1}due to TTP and phthalates, lose intensity or are not detectable by ATR-FTIR after artificial aging. The signals at 1460 cm^{-1} in CAB and at 900 cm^{-1} in CAP and CAB decrease, while no substantial variations are discernible in CA within these regions. The band at 1590 cm^{-1} is masked by the shoulder that has formed at 1600 cm^{-1} during artificial aging, and its evolution cannot be deduced.

The findings suggest a relationship between the alterations in color and the macroscopic deterioration of the material, as well as the chemical degradation (predominantly chain breakage) and physical (loss-migration of additives) changes in CA [48,49].

The impact of climate artificial aging with RH/T (Figure S5) was found to be significantly less pronounced than that of radiation. The acetates exhibited different behaviors, with CAB and CAP demonstrating stability, exhibiting only minor chemical changes and macroscopically imperceptible physical changes. This is likely attributable to their reduced water absorption, due to their higher hydrocarbon nature and the type and amount of plasticizer employed [50]. Conversely, CA exhibited a 7 % contraction and a 2 % mass reduction, potentially attributable to evaporation of the plasticizer and loss of elasticity, a hypothesis substantiated by the decline in the 1598 and 1579 cm^{-1} bands assigned to plasticizers in

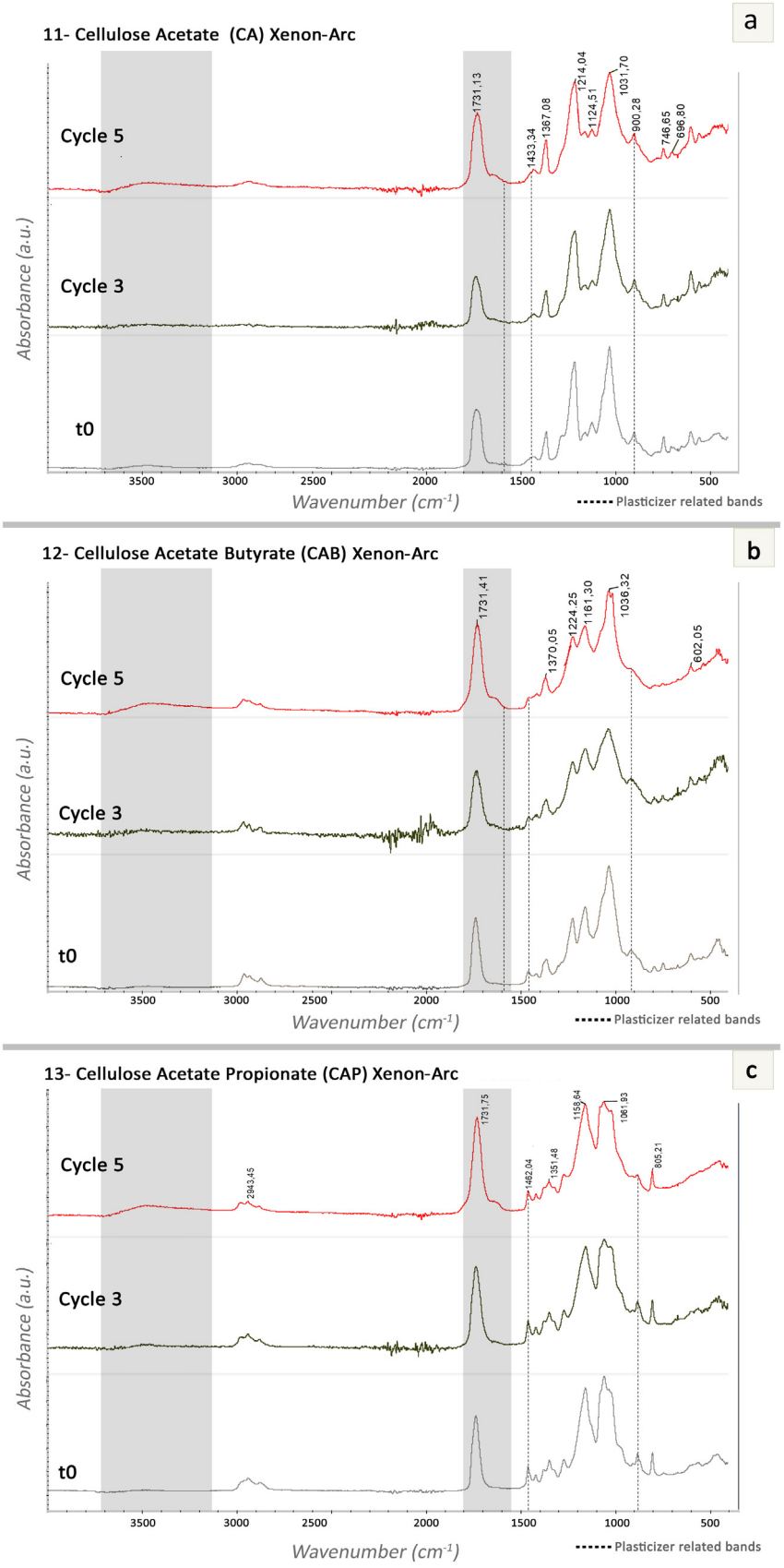

Fig. 10. Composition study versus artificial aging time; Comparison of ATR-FTIR spectra in Xenon-Arc (initial, intermediate and final time). a) CA, b) CAB and c) CAP.

the final cycle [34]. By contrast, a decline in the intensity of the signal in three bands at 1731 cm^{-1} (C=O), 1278 cm^{-1} (COC) and 1125 cm^{-1} (CO), associated with the vibrations of the ester and ether bonds, is also observed, suggesting partial de-esterification by hydrolysis and alteration of the chain, indicating the onset of degradation. The deacetylation of the molecule occurs by reaction between water and an acetyl group, resulting in its substitution by an hydroxyl group and the formation of acetic acid as a by-product of decomposition [19,38,49].

5. Conclusions

The creation of a freely accessible online database represents the main contribution and innovation of this work. This resource compiles, systematizes, and makes available a large set of reference data on polymeric materials relevant to conservation, restoration, and artistic production. Beyond serving as a repository, the database allows for the visualization, comparison, and joint interpretation of results, greatly facilitating the recognition and characterization of polymers-especially those that have undergone degradation or artificial aging. It thus provides an open, structured, and accessible source of information that supports the interpretation of complex data and the design of long-term preservation strategies.

The experimental methodology developed in this study, based on the analysis of fundamental physical and chemical properties, ensures the generation of consistent and comparable data for inclusion in the database. While not the most innovative aspect, it has proven effective for characterizing materials and predicting their long-term behavior. The study of PVCs and cellulose acetates demonstrated that these materials are particularly sensitive to artificial aging under Xenon-Arc radiation compared to humidity-temperature conditions, showing a general loss of plasticizers and polymer chain degradation.

Overall, the database stands as a valuable and dynamic tool that not only supports heritage conservation but also encourages future research and the development of new, more compatible materials and conservation strategies.

Formatting of funding sources

This work was supported by the research project PR27/21-013 Universidad Complutense of Madrid and Community of Madrid.

Acknowledgements

The authors thank the assistance of the research centers from Complutense University of Madrid (CAI) for the Thermal analysis and Py-GC-MS measurements.

Supplementary materials

Supplementary material associated with this article can be found, in the online version, at doi:10.1016/j.culher.2025.12.013.

References

[1] S.G. Fernández-Villa, Plastics in Art and Design Until 1945: History, Technology, Conservation and Identification, University Complutense of Madrid, Madrid, 2010.
[2] M. Lazzari, D. Reggio, What fate for plastics in artworks? an overview of their identification and degradative behaviour, Polymers 13 (883) (2021) 3–22.
[3] F. Waentig, Plastics in Art. A study from the Conservation Point of View, Michael Imhof Verlag, Petersberg, 2008.
[4] P. Walters, D.F. Cadogan, C.J. Howick, Plasticizers," in *Ullmann's Encyclopedia of Industrial Chemistry*, Wiley-VCH, Weinheim, 2020.
[5] Ministerio de Cultura-Gobierno de España, "POLYEVART," 2011 [Online].. Available: https://www.cultura.gob.es/cultura/areas/patrimonio/mc/polyevart/presentacion.html [Accessed 21112024].
[6] R. Chércoles, M. San Andrés, J.M. De la Roja, M.L. Gómez, Analytical characterization of polymers used in conservation and restoration by ATR-FTIR spectroscopy, Anal. Bioanal. Chem. 395 (2009) 2081–2096.
[7] C. Cucci, G. Bartolozzi, V. Marchiafava, M. Picollo, E. Richardson, Study of semi-synthetic plastic objects of historic interest using non-invasive total reflectance FT-IR, Microchem. J. (124) (2016) 889–897.
[8] B. Keneghan, Identification of plastics in cultural heritage collections by Fourier transform infrared spectroscopy (FTIR), Anal. Methods (10) (2018) 687–689.
[9] L. Ascione, M.C. Mistretta, M. Pedeferri, F.P. La Mantia, Effect of environmental conditions on the durability of polycarbonate for the protection of cultural heritage sites, J. Appl. Biomater. Funct. Mater. 4 (17) (2019) Journal of Applied Biomaterials & Functional Materials.
[10] E. Aura-Castro, C. Díaz-Marín, X. Mas-Barberà, M. Sánchez López, E.Vendrell Vidal, Characterization of 3d printing filaments applied in restoration of sensitive archaeological objects using rapid prototyping, Rapid. Prototyp. J. 4 (27) (2021) 645–657.
[11] POPART project, "POPART: preservation of plastic ARTefacts in museum collections," 2012 [Online].. Available: https://popart-highlights.mnhn.fr [Accessed 15032025]..
[12] M. San Andrés, M. Baonza, O. Montoro, A. Bouzas, R. Chércoles, M. Taravillo, J.M. De, La Roja, Analytical approach by Raman Spectroscopy, International Congress on the Application of Raman Spectroscopy in Art and Archeology, 2013 Ljubljana.
[13] R. Chércoles, M. San Andrés, J.M. De la Roja, M. Gómez, Analisys polimeric materials methodology used in preventive conservation, VI Congress of IIC Spanish group IIC (GEIIC), 2018 Vitoria.
[14] S. Vahur, K. Virro, I. Leito, Web-based infrared spectral databases relevant to conservation, J. Can. Assoc. Conserv. 30 (2005) 10–17.
[15] V.Martínez Marín, On the concepts of film preservation, conservation, and restoration: the case of the Cineteca Nacional de México through the approach of Paolo Cherchi Usai, Rev. Int. Conserv. Restaur. Museol. 11 (22) (2020) 34–57.
[16] B. Lavedrine, A. Fournier, G. Martin, Physical and chemical processes leading to deterioration of plastics, in: Preservation of Plastic Artefacts in Museum Collections, Comité des Travaux Historiques et Scientifiques, Paris, 2012, pp. 162–167.
[17] T. Krieg, C. Mazzon, E. Gómez-Sánchez, Material analysis and a visual guide of degradation phenomena in historical synthetic polymers as tools to follow ageing processes in industrial heritage collections, Polymers 14 (121) (2022) 1–58.
[18] R.Chércoles Asensio, Study About Physical-Chemical Behavior of Polymeric Materials Used in Conservation and Restoration of Cultural Heritage, University Complutense of Madrid, Madrid, 2016.
[19] A. Del Amo Garcia, Clasificar Para Preservar [To Classify in Order to Preserve], Instituto de la Cinematografía y de las Artes audiovisuales, Madrid, 2006.
[20] E. Arrington and R. Kehl, "Process for making a cellulose triacetate photographic film base". USA Patent US5529737A, 1996.
[21] M. Edge, N.S. Allen, M. Hayes, P.N. Riley, C.V. Horie, J. Luc-Gardete, Mechanisms of deterioration in cellulose nitrate base archival cinematograph film, Eur. Polym. J. 26 (6) (1990) 623–630.
[22] S.G. Fernández-Villa, R. Chércoles Asensio, M.San Andrés, in: Effectiveness Evaluation of Molisch's Test for the identification of Historical Cellulose Plastics, The Plastics Heritage Congress, Lisboa, 2019, pp. 211–224.
[23] G.M. Melgosa, M.M. Pérez, A. Yebra, R. Huertas, Some reflections and recent international recommendations on color-difference evaluation, Opt. Pura Apl. (34) (2001) 1–10.
[24] B. Lavédrine, A. Fournier, G. Martin, Preservation of Plastic Artefacts in Museum Collections, Comité des Travaux Historiques et Scientifiques-CTHS, Paris, 2012.
[25] J. Pospilsil, Z. Horak, J. Pilar, N. Billingham, H. Zweifel, S. Nespurek, Influence of testing conditions on the performance and durability of polymer stabilisers in thermal oxidation, Polym. Degrad. Stab. 8 (2) (2003) 145–162.
[26] T.T. Schaffer, Effects of Light on Materials in Collections, Getty Publications, Los Angeles, 2002.
[27] L.F.E. Jacques, Accelerated and outdoor/natural exposure testing of coatings, Prog. Polym. Sci. 25 (9) (2000) 1337–1362.
[28] M. Yufeng, L. Shengliang, L. Qiaoguang, G. Qian, J. Puyou, Z. Yonghong, Physical and chemical modifications of poly(vinyl chloride) materials to prevent plasticizer migration - still on the run, Reactive and Functional Polymers, 147, 2020.
[29] Y.R. Shashoua, Inhibiting the Deterioration of Plasticized Poly (Vinyl Chloride): a Museum Perspective, Technical University of Denmark, Department of Chemical and Biochemical Engineering, 2001.
[30] M. Gilbert and S. Patrick, "Chapter 13 - poly(vinyl chloride)," in *Plastics Materials Brydson*, Butterworth-Heinemann, 2016, pp. 311–362.
[31] P. Dunn, B.C. Ennis, Thermal analysis of compounded poly (vinyl chloride), J. Appl. Polym. Sci. 14 (1970) 355–364.
[32] M. Beltran, A. Marcilla, PVC plastisols decomposition by FTIR spectroscopy, Eur. Polym. J. 33 (8) (1997) 1271–1280.
[33] É.C. Roldao, A Contribution for the Preservation of Cellulose Esters Black and White Negatives, Universidad de Ciencias y Tecnología, Lisboa, 2018.
[34] M.R. Schilling, M. Bouchard, H. Khanjian, T. Learner, A. Phenix, R. Rivenc, Application of chemical and thermal analysis methods for studying cellulose ester plastics, Acc. Chem. Res. 6 (43) (2010) 888–896.
[35] D.M. Furlan Sandrini, D. Lury Morgado, A.J. de Oliveira, D.A. de Moraes, L.C. Varanda, E. Frollini, Cellulose esters: synthesis for further formation of films with magnetite nanoparticles incorporated, Int. J. Biol. Macromol. 264 (130594) (2024).

[36] M.Truffa Giachet, M. Schilling, K. McCormick, J. Mazurek, E. Richardson, H. Khanjian, Assessment of the composition and condition of animation cels made from cellulose acetate, Polym. Degrad. Stab. 107 (2014) 223–230.
[37] J.L. Bigourdan, Preservation of acetate base motion-picture film: from stability studies to film preservation in practice, The Vinegar Syndrome: a Handbook, Prevention, Remedies and the Use of New Technologies, The GAMMA Group, Bologna, 2000.
[38] I.R. Ahmad, D. Cane, J.H. Townsend, C. Triana, L. Mazze, K. Curran, Are we overestimating the permanence of cellulose triacetate cinematographic films? A mathematical model for the vinegar syndrome, Polym, Degrad, Stab. 172 (2020) 109050.
[39] J.M. Reilly, IPI Storage Guide for Acetate Film, Image Permanence Institute, Rochester, 1993.
[40] A. Bonifacio, L. Bonetti, E. Piantanida, L. De Nardo, Plasticizer design strategies enabling advanced applications of cellulose acetate, Eur. Polym. J. 197 (112360) (2023).
[41] M.K. McGath, Investigation of Deterioration Mechanisms of Cellulose Acetate Compounded with Triphenyl Phosphate, University of Arizona, Tucson, 2012.
[42] S. Patrick, PVC Practical Guide to Polyvinyl Chloride, Rapra Technology Limited, Shrewsbury, 2005.
[43] Y. Shashoua, Plastics in collections, in: Conservation of Plastics : Materials Science, Degradation and Conservation, Butterworth-Heinemann, Oxford, 2008, pp. 1–19.
[44] J. Lacoste, D. Carlsson, S. Falicki, D. Wiles, Polyethylene hydroperoxide decomposition products, Polym. Degrad. Stab. 34 (1–3) (1991) 309–323.
[45] D. Nishimura, Strategies for the storage of cellulose acetate film, Top. Photogr. Preserv. 16 (2015) 239–244.
[46] E. Richardson, in: The Physical Effects of Plasticizer Loss in Cellulose Acetate Films, POPArtRT: Preservation of Plastic ARTifacts in Museum Collections, Paris, 2012, pp. 196–198.
[47] L. Liu, D. Gong, L. Bratasz, Z. Zhu, C. Wang, Degradation markers and plasticizer loss of cellulose acetate films during ageing, Polym. Degrad. Stab. 168 (108952) (2019).
[48] K. Curran, M. Strlič, Polymers and volatiles: using VOC analysis for the conservation of plastic and rubber objects, Stud. Conserv. 60 (30) (2015) 1–14.
[49] T.A. Ram, Archival preservation of photographic films-a perspective, Polym. Degrad. Stab. 29 (1) (1990) 3–29.
[50] J. Rychlý, L. Rychlá, Physical and chemical processes leading to deterioration of original porperties of plastics, in: Preservation of Plastic Artefacts in Museum Collections, Comité des Travaux Historiques et Scientifiques, Paris, 2012, pp. 162–167.